Published in final edited form as:
Shock. 2011 September ; 36(3): 295–302. doi:10.1097/SHK.0b013e318225ad7e.

The hydroxylase inhibitor DMOG attenuates endotoxic shock via alternative activation of macrophages and IL-10 production by B-1 cells

Emily Hams[*], **Sean P. Saunders**[*], **Eoin P. Cummins**[†], **Aisling O'Connor**[†], **Murtaza T. Tambuwala**[†], **William M. Gallagher**[†], **Annette Byrne**[†], **Antonio Campos-Torres**[‡], **Paul M. Moynagh**[‡], **Christian Jobin**[§], **Cormac T. Taylor**[†,2], and **Padraic G. Fallon**[*,1,2,3]

[*]Institute of Molecular Medicine, Trinity College Dublin, Ireland [†]UCD Conway Institute, University College Dublin, Ireland [‡]Institute of Immunology, National University of Ireland Maynooth, Ireland [§]Department of Medicine, Microbiology/Immunology, Pharmacology, The University of North Carolina, USA

Abstract

Localized tissue hypoxia is a feature of infection and inflammation, resulting in the upregulation of the transcription factors HIF-1α and NF-κB via inhibition of oxygen sensing hydroxylase enzymes. Previous studies have demonstrated a beneficial role for the hydroxylase inhibitor dimethyloxallyl glycine (DMOG) in inflammatory conditions, including experimental colitis, by regulating the activity of HIF-1 and NF-κB. We have demonstrated *in vivo* that pre-treatment with DMOG attenuates systemic LPS-induced activation of the NF-κB pathway. Furthermore, mice treated with DMOG had significantly increased survival in LPS-induced shock. Conversely, in models of polymicrobial sepsis, DMOG exacerbates disease severity. DMOG treatment of mice promotes M2 polarization in macrophages within the peritoneal cavity, resulting in the downregulation of pro-inflammatory cytokines such as TNFα. In addition, *in vivo* DMOG treatment upregulates IL-10 expression, specifically in the peritoneal B-1 cell population. This study demonstrates cell type specific roles for hydroxylase inhibition *in vivo* and provides insight into the mechanism underlying the protection conveyed by DMOG in models of endotoxic shock.

Keywords

LPS; hypoxia; mouse; NF-κB; tolerance

Introduction

Sepsis is a complex condition characterized by a systemic bacterial infection, which can result in septic shock and multi-organ failure. Despite the use of broad-spectrum antibiotics and improvements in care, sepsis is still associated with a mortality rate of between 30% and 50% in severe cases (1, 2). The immunopathogenesis of sepsis is associated with overwhelming systemic inflammation and suppression of the adaptive immune response. Recent work has identified a high degree of crosstalk between oxygen sensing pathways,

[3]Address correspondence and reprint request: Dr Padraic Fallon, Institute of Molecular Medicine, St. James's Hospital, Trinity College Dublin, Dublin 8, Ireland. pfallon@tcd.ie Phone: +353 1 896 3267; Fax: 353 1 896 4040.
[1]This work was supported by Science Foundation Ireland and Health Research Board.
[2]Joint Authorship.

responsible for adaptation to hypoxia, and regulators of innate immunity and inflammation (3). Central to the interplay between hypoxia and the innate response are the hypoxia-inducible factors (HIFs) the oxygen-sensitivity of which is conferred by a family of O_2-dependent hydroxylases (4). Hypoxia also activates the master regulator of innate immunity and inflammation, NF-κB through decreased hydroxylase activity (5). A high degree of crosstalk between NF-κB and HIF signaling exists. For example, pro-inflammatory mediators such as lipopolysaccharide (LPS) increase HIF mRNA expression in macrophages (MØ) through activation of NF-κB pathways (6, 7). Conversely, NF-κB activation via HIF has been reported in neutrophils (8).

In the context of sepsis, important roles for both HIF and NF-κB have been described in the development of LPS-induced endotoxemia, with a *hif1α* deletion in the myeloid lineage protective against LPS-induced mortality *in vivo* (9, 10). In addition, hypoxia is a feature in chronic inflammatory conditions including rheumatoid arthritis, psoriasis and inflammatory bowel disease (11-13). In various inflammatory conditions the use and development of prolyl-hydroxylase inhibitors, such as dimethyloxallyl glycine (DMOG), in the treatment of disease is showing some benefits, particularly in models of inflammatory bowel disease (13, 14).

Data presented herein will further address the role of inhibiting hydroxylases in the progression of the innate response to LPS challenge. We identify the ability of the hydroxylase inhibitor DMOG to attenuate LPS induced NF-κB signaling *in vivo* and show DMOG induced tolerance to subsequent LPS challenge and promotes M2 MØ polarization. We also clearly show the ability of DMOG to upregulate IL-10 expression in models of sepsis and propose that both mechanisms may play important roles in the protective *in vivo* effects of hydroxylase inhibition in LPS-driven endotoxemia.

Materials and Methods

Animals

BALB/c and C57BL/6 mice were purchased from Harlan (Bicester, U.K.) and Charles River respectively. NF-κB-RE-luc (Oslo) mice, which carry a transgene containing 3 NF-kB responsive element (RE) sites from the Igκ light chain promoter and a modified firefly luciferase cDNA (Promega pGL-3) on a BALB/c background, were obtained from Caliper LifeSciences (Hopkinton MA, USA). IL-10-eGFP reporter mice (15) on a C57BL/6 background were obtained from Jackson Laboratories (Bar Harbor ME, USA), and subsequently backcrossed to BALB/c strain in-house. IL-$10^{-/-}$ and RAG-$1^{-/-}$ mice were from Jackson Laboratories (Bar Harbor ME, USA) and bred in-house. $NF\kappa B^{EGFP}$ reporter mice (16) were bred in-house. NF-κB $p50^{-/-}$ were purchased from Jackson Laboratories (Bar Harbor ME, USA). Animals were housed in a specific pathogen-free facility in individually ventilated and filtered cages under positive pressure. All animal experiments were performed in compliance with Irish Department of Health and Children regulations and approved by the Trinity College Dublin's BioResources ethical review board.

Induction of LPS-induced shock

Endotoxin shock was induced in mice via intraperitoneal (i.p.) injection of ultrapure lipopolysaccharide (LPS) extracted from *E. coli* (Invivogen, France) at a dose of 10 mg/kg (17). DMOG (Cayman Chemical, USA) was prepared with sterile water and screened for endotoxin contamination (Chromogenic LAL, Biowhittaker, MD) with < 0.01 EU detected per mg. Mice were injected with DMOG (8 mg/mouse) i.p (13), 2 hours prior to LPS treatment. Animals were assessed as described (17), and scored at hourly intervals using the following criteria: score 0 – no symptoms; score 1 – piloerection, huddling; score 2 –

piloerection, huddling, diahorrea; score 3 – lack of interest in surroundings, severe diahorrea; score 4 – decreased movement, listless appearance; and score 5 – loss of self-righting reflex. When mice reach score 5 they were humanely killed. To assess the potential role of IL-10, anti-IL-10R mAb (Clone 1B1.3a; ATCC, Manassas VA, USA), prepared as described (18), was administered i.p. (500 μg) to mice 3 hours prior, or 3 hours, after LPS treatment.

Induction of CLP-mediated sepsis

Surgically-induced polymicrobial sepsis was introduced in mice using the cecal ligation and puncture (CLP) method. Briefly, the mice were anaesthetized and a small section of the cecum ligated and punctured using a 21-guage needle to allow leakage of the cecal contents into the peritoneum. After surgery 1 ml of sterile NaCl was administered sub-cutaneously. Groups of mice were given DMOG (8 mg/mouse) intraperitoneally 2 hours prior to surgery and every 24 hours subsequently. A sham group of mice received surgery without CLP. The mice were allowed to recover and scored every 12 hours using the criteria for LPS-induced endotoxemia, as above. Blood was collected for serum cytokine analysis 3 days after surgery. Pain relief was provided throughout using buprenorphine.

In vivo M2 macrophage activation

Chitin (Sigma) was washed 3 times and prepared in PBS by sonication 3 times for 15 seconds on ice. This was filtered using 70 μM filters and the filtrate used for subsequent immunization. Approximately 800 ng was administered i.p. both alone, and in combination with DMOG (8 mg/mouse). Peritoneal cells were collected by lavage after 48 hours and cDNA prepared for real-time PCR analysis, as outlined below.

In vivo imaging

Mice ubiquitously expressing a transgene encoding firefly luciferase under the control of a concatomer of NF-kB response elements (Caliper LS) were given LPS and DMOG, as outlined above. Following treatment the mice were anesthetized and injected i.p. with luciferin (150 mg/kg). *In vivo* luciferase activity (indicative of NF-kB activation), measured as photons/sec/cm2/steradien, was quantified using Living Image Software (V. 3.0.2; Caliper LS).

Cytokine ELISAs and multiplex cytokine analysis

Supernatants from *in vitro* cultures and mouse serum were analyzed by sandwich ELISAs to quantify levels of specific cytokines. All cytokines (IL-1β, IL-6, IL-10 and TNFα) were measured with the DuoSet ELISA development system from R&D Systems following the manufacturers protocol. Multiplex analysis was performed on serum samples from affected mice using the pro-inflammatory 7-plex plate from Meso Scale Discovery (Meso Scale Discovery, MD, USA), which measures IL-1β, IL-6, IL-8, IL-10, IL-12p70, IFN-γ and TNFα. The protocol was followed as described in the manufacturers instructions.

Flow cytometry

Surface marker expression and detection of IL-10-eGFP^{+} and NFκB-eGFP^{+} cells were assessed by flow cytometry with data collection on a CyAn (Beckman Coulter). Data were analyzed using FlowJo software (Tree Star). Cells were stained with eBiosciences mAbs; PerCP anti-CD4 (RM4-5), Pe-Cy7 anti-CD11c (N418), APC anti-F4/80 (BM8), APC anti-B220 (RA3-6B2) and Pacific Blue anti-CD19 (eBio1D3). BD Biosciences mAbs; PE anti-CD5 (53-7.3) and PE anti-CD11b (M1/70). Flow buffers used contained 2mM EDTA to exclude doublets. Using appropriate isotype-controls, quadrants were drawn and data plotted on logarithmic scale density- or dot-plots.

Isolation and culture of peritoneal macrophages and B1 cells

Peritoneal MØ were isolated as described (17). In brief, the peritoneal cavity was lavaged with 5 ml ice cold PBS. The resulting cells were washed and resuspended in RPMI 1640 (Invitrogen Life Technologies) supplemented 2 mM L-glutamine, 100 U/ml penicillin, and 100 μg/ml streptomycin at a density of 2×10^6 cells/ml. Cells were incubated at 37°C and 5% CO_2 for 2 hours and any non-adherent cells removed. The remaining adherent cells were stimulated with DMOG (1 mM) 2 hours prior to stimulation with LPS (10 μg/ml) for between 5 and 30 minutes, after which cells were collected for protein extraction. In addition, adherent peritoneal cells were cultured for 2 hours with DMOG (1 mM) followed by subsequent stimulation with either LPS(10 μg/ml) and IFNγ (10 ng/ml), GM-CSF (10 ng/ml), IL-4 (10 ng/ml) and IL-13 (10 ng/ml) or IL-10 (10 ng/ml). After an18 hour incubation, cells were collected and cDNA prepared for subsequent real-time PCR.

B1 cells were FACS sorted from total peritoneal cells using positive selection of Pacific blue anti-$CD19^+$ (eBio1D3) and PE anti-$CD5^+$ (53-7.3) cells. Cells were cultured at 5×10^6 cells/ml in the presence of DMOG (1 mM) for 2 hours followed by stimulation with LPS (10 μg/ml) for 15 and 30 minutes, after which cells were collected for protein extraction.

RNA isolation and real-time PCR

RNA was isolated from peritoneal exudate cells using the RNeasy kit and reverse transcribed using the Quantitect reverse transcription kit incorporating a genomic DNA elimination step (QIAGEN). Real-time quantitative PCR was performed on an ABI Prism 7900HT sequence detection system (Applied Biosystems) using pre-designed TaqMan gene expression assays specific for murine iNOS (Mm00440485_m1), Arginase-1 (Mm00475988_m1), Relm-α (Mm00445109_m1) and YM1 (Mm00657889_m1). Specific gene expression was normalized to murine GAPDH. Fold expression was calculated using the ΔΔCT method of analysis (Applied Biosystems).

Protein extraction and immunoblotting

Whole cell extracts were prepared from peritoneal MØ following cell lysis in RIPA lysis buffer. Protein concentrations of the samples were quantified using the commercially available BCA kit (Thermo Scientific). Cell extracts (10 μg) were separated by SDS-PAGE on 12% polyacrylamide gels and transferred to PVDF membrane (Millipore). Membranes were probed with rabbit polyclonal antibodies specific for total (H-119) and phosphorylated-p50 (Ser 337), total (C-20) and phosphorylated-p65 (Ser 311), total (48H2) and phosphorylated-CREB (Ser 133) and GAPDH (D-6), followed by incubation with an HRP-conjugated goat anti-rabbit secondary antibody (Dako). Immunolabelled proteins were visualized by chemiluminescence using the ECL detection system (Millipore). Quantification of protein expression from 3 blots representative of 3 individual experiments was performed by densitometry using ImageJ software.

Statistics

Statistical analysis was performed using GraphPad InStat®. Results are presented as mean ± SEM. Differences, indicated as two-tailed *P* values, were considered significant when $P>0.05$ as assessed by unpaired Student's *t* test with Welch correction applied as necessary, or LogRank correlation for survival statistics.

Results

DMOG pre-conditioning promotes basal but inhibits LPS-induced NF-κB activity

We have previously demonstrated using cell lines that pharmacologic or genetic inhibition of HIF hydroxylases leads to activation of NF-κB signalling (5). While the regulation of NF-κB by hydroxylases has been confirmed both *in vitro* and *in vivo* (6, 19-21), specific mechanisms and targets remain unknown. In addition there is little existing data on the regulatory role of hydroxylases in controlling NF-kB activation by innate immune receptors such as TLRs. With this in mind, we evaluated the interplay between hydroxylases and the TLR4 signaling pathway as activated by LPS. Following *in vivo* treatment of $NF\kappa B^{EGFP}$ mice with the hydroxylase inhibitor DMOG, there is activation of basal NF-κB in peritoneal MØ, neutrophils and B cells (Fig. 1; Supplemental Fig. 1). Paradoxically, while LPS treatment evoked NF-κB activation of peritoneal cell populations, cells from mice pre-treated with DMOG prior to LPS exposure demonstrated significantly (*P<0.05-0.01*) lower NF-κB activity (Fig. 1). This led us to hypothesize that the low degree of NF-κB activation induced by DMOG leads to a pre-conditioning effect that renders these cells tolerant to subsequent LPS exposure, similar to reported mechanisms of LPS tolerance (22). Due to the ability of DMOG-alone to activate NF-κB we tested for endotoxin contamination (detected <0.01 Endotoxin Units per mg) and confirmed DMOG activation of NF-κB is independent of TLR4 using cells from $TLR4^{-/-}$ mice (data not shown). To test this hypothesis *in vivo*, LPS-induced endotoxic shock was evoked in mice expressing luciferase under the control of a concatomer of NF-κB response elements, both with and without prior DMOG treatment, and activation of NF-κB was monitored by *in vivo* imaging. Consistent with the peritoneal cell data described above (Fig. 1), LPS treatment induced systemic NF-κB activity, which was significantly reduced in mice pre-treated with DMOG (Fig. 2). These data were quantified by *in vivo* luminometry and demonstrate a significant (*P<0.01*) reduction in systemic NF-κB activity in DMOG pre-treated mice compared to mice treated with LPS-alone (Fig. 2). Previous work by the group has assessed the activation of NF-κB in response to i.p. administration of LPS and found systemic activation affecting all organs (5, 13, 23). These data promoted the hypothesis that DMOG pre-treatment induces a mild NF-κB activation *in vivo* which tolerizes mice to subsequent LPS challenge, with decreased systemic NF-κB activation.

DMOG treatment ameliorates LPS-mediated endotoxin shock

We next investigated the *in vivo* consequences of DMOG treatment of mice before LPS-induced endotoxin shock. Mice were pre-treated mice with DMOG for 2 hours prior to LPS administration to induce endotoxin shock. In mice treated with LPS-alone, signs of disease peaked at 12 hours (data not shown) and all mice were dead by 72 hours (Fig. 3A). In mice pre-treated with DMOG there was marked delayed disease onset with a significant (*P<0.05*) reduction in LPS-induced mortality (Fig. 3A). This protective effect of DMOG was associated with significantly (*P<0.05*) decreased levels of the acute phase protein, serum amyloid A (SAA; Fig. 3B) and the pro-inflammatory cytokine TNFα (Fig. 3C). LPS-induced IL-1β and IL-6 were not attenuated with prior DMOG treatment (Fig. 3D, E). In contrast to TNFα, DMOG-treated mice had significantly enhanced (*P>0.05*) LPS-induced expression of the anti-inflammatory cytokine IL-10 compared to mice treated with LPS alone (Fig. 3F). It is noteworthy that when mice were treated with DMOG after LPS injection, the inhibitor had no effect on the development of the endotoxic shock (data not shown). Therefore, *in vivo* pretreatment of mice with DMOG protects mice from LPS-induced shock.

DMOG promotes macrophage M2 polarization

MØ are the predominant cell type in the peritoneal cavity and play an important role in the initial response to LPS. LPS stimulation evokes classical (M1) activation of MØ (24), however, it has previously been shown that activation of the alternative (M2) macrophage phenotype, is associated with LPS tolerance (25). Due to the apparent tolerizing role for DMOG in attenuating NF-κB activation in response to LPS, we assessed the potential for DMOG to drive M1 or M2 polarization *in vivo*. Mice were injected i.p. with LPS or M2 phenotype inducing chitin (26), and the relative expression of M1 (iNOS; Fig. 4A) and M2 (Arginase-1, Relm-α, YM1; Fig.4B) markers on peritoneal MØ were analyzed by qPCR. In mice treated with chitin, YM1, Arginase-1 and Relm-α were significantly elevated ($P<0.05$) compared to control PBS-injected mice, consistent with generation of an M2 polarization (26). DMOG treatment with chitin significantly ($P<0.05$-0.01) enhanced the levels of M2 genes (Fig. 4B). Conversely, although peritoneal MØ isolated from mice treated with DMOG- alone showed an upregulation of the M1 marker iNOS, expression is significantly decreased in mice treated with DMOG and LPS compared to mice treated with LPS alone (Fig. 4A). To further confirm that DMOG induced M2 cell expansion, we used an *in vitro* model and exposed peritoneal MØ to DMOG, followed by GM-CSF or a combination of LPS and IFNγ to drive M1 polarisation, and IL-10 or a combination of IL-4 and IL-13 to drive M2 polarisation (Figures 4C and 4D). Consistent with the *in vivo* data, in an *in vitro* system DMOG inhibited MØ polarization to an M1 phenotype (Figure 4C), while promoting M2 polarisation (Figure 4D).

While these data are indicative that DMOG enhances M2 cell expansion *in vivo* in response to chitin, and also *in vitro*, which is consistent with DMOG evoking a state of LPS tolerance, it does not fully define the mechanism. It has recently been shown that activation of the p50 NF-κB subunit can inhibit M1 and drive M2 macrophage activation, a phenotype that is associated with LPS tolerance (27). Therefore, p50 activation in peritoneal MØ treated with DMOG and/or LPS were tested. There was an upregulation of phosphorylated p50 (S337) in MØ treated with DMOG alone and levels are further increased 5 minutes after cells are additionally treated with LPS (Fig. 5A, B). In contrast there was no difference in phosphorylation of the p65 NF-κB subunit, which would be more associated with classical M1 activation (Fig. 5A, B). To confirm these *in vitro* observations, we induced endotoxic shock with and without DMOG treatment in p50 deficient mice. While DMOG protected WT mice from LPS-induced endotoxic shock, DMOG did not reduce mortality of LPS-treated $p50^{-/-}$ mice (Fig. 6A). In addition, while DMOG modulated the serum levels of TNFα and IL-10 in WT mice, it had no effect on these cytokines in LPS-treated $p50^{-/-}$ mice (Fig. 6B). Furthermore, RT-PCR analysis of the peritoneal cells from $p50^{-/-}$ mice showed no upregulation of any of the typical genes associated with M2 macrophage polarization, consistent with the importance of p50 in generating an M2 phenotype (data not shown). As DMOG inhibits prolyl-hydroxylases we also looked at the expression of HIF1α in response to DMOG and LPS in peritoneal macrophages. As expected, stimulation of the cells with DMOG resulted in an increase in HIF1α and HIF2, with no apparent effect of LPS (data not shown). These data are consistent with DMOG treatment inducing tolerance to LPS via upregulation of p50 NF-κB and an expansion of M2 cells.

IL-10 receptor blockade ameliorates the protective role of DMOG in endotoxic shock

DMOG increased serum levels of the anti-inflammatory cytokine IL-10 after LPS treatment (Fig. 3F, 6A). To determine if the elevated IL-10 levels induced by DMOG were relevant to the protective effects of DMOG in LPS-induced endotoxic shock, we used a mAb to block the IL-10 receptor (IL-10R) *in vivo*. Prior to LPS challenge, the anti-IL-10R mAb was injected to mice either alone or in combination with DMOG. While DMOG alone rendered mice refractory to LPS-induced mortality, co-treatment with anti-IL-10R mAb blocked the

protective effects of DMOG on disease severity, with 100% mortality observed at 12 hours following induction of sepsis, compared with 0% mortality seen in mice treated with DMOG and LPS alone (Fig. 7A). In mice treated with anti-IL-10R mAb there was comparable LPS-induced death as DMOG plus mAb treated mice (Fig. 7A). The effects of blocking IL-10 signaling with DMOG treatment were only functional when anti-IL-10R mAb was administered prior to treatment. Mice treated with anti-IL-10R mAb 3 hours following DMOG and LPS challenge had a comparable response as mice treated with LPS alone (data not shown). Serum cytokine levels were quantified at 3 hours following LPS exposure (Fig. 7B-C). Similar to earlier studies (Fig. 3), DMOG treatment decreased levels of TNFα and increased IL-10 expression in response to LPS (Fig. 3B-C). Anti-IL-10R mAb treatment increased TNFα expression, which was reduced in response to DMOG treatment (Fig. 7B). IL-10 expression is also increased in response to anti-IL-10R blockade, consistent with accumulation of IL-10 after blocking of its receptor (Fig. 7C). However, IL-10 expression is significantly ($P<0.05$) increased after additional treatment with DMOG (Fig. 7C), confirming DMOG evokes IL-10 release. Furthermore, this essential role for IL-10 in DMOG-mediated protection from LPS-induced shock was confirmed with IL-$10^{-/-}$ animals (data not shown).

To formally define the cellular source of IL-10 in DMOG treated mice we initially induced LPS-mediated shock in both untreated and DMOG-treated RAG-$1^{-/-}$ mice, which lack T and B cells. While DMOG-treated wild-type mice were tolerant to LPS induced shock, treatment of RAG-$1^{-/-}$mice with DMOG caused no alteration in severity (data not shown). Consistent with DMOG stimulating IL-10 release from a T or B lymphocyte source, DMOG-treated RAG-$1^{-/-}$ mice had comparable IL-10 expression as untreated mice (Fig. 8A). To further define the cellular source of IL-10, we used IL-10eGFP mice to determine IL-10eGFP expression in peritoneal MØ, B-1 and B-2 cells (Fig. 8B, Supplemental Fig. 2). DMOG treatment of mice significantly ($P<0.05$) enhances LPS-induced IL-10eGFP expression by peritoneal B-1 cells, a known cellular source of IL-10 in LPS challenge (28), but not by MØ or B-2 cells (29, 30), indicating for the first time a cell type-specific effect of DMOG (Fig. 8B).

CREB has been implicated in regulating genes associated with inflammation, including IL-10, and also hypoxia, so could provide one potential mechanism linking the effects of DMOG in systemic inflammation. Analysis of *in vitro* CREB activation in the peritoneal B-1 cell population shows upregulation of phosphorylated CREB in response to treatment with DMOG (Fig. 8C, D), which may explain one potential mechanism by which DMOG is acting. This effect appears to be cell specific, as peritoneal macrophages do not show any significant activation of CREB in response to DMOG (Fig. 8C, E).

DMOG treatment during polymicrobial sepsis is associated with increased disease severity

To assess the efficacy of DMOG in a clinical sepsis model, we used the cecal ligation and puncture model in both untreated, and mice treated with DMOG. Following CLP in untreated mice there are signs of disease within 12 hours post surgery of compared to sham-operated mice, with death of animals occurring within 7 days of surgery (Fig. 9A). However, mice receiving DMOG treatment prior to surgery develop significant exacerbation of disease symptoms and demonstrate a significantly ($P<0.01$) increased mortality rate when compared to those receiving surgery-alone, with 100% mortality at 96 hours post surgery (Fig. 9A). However, serum cytokine analysis also shows a decrease in TNFα and increase in IL-10 in mice treated with DMOG (Fig. 9B), consistent with the effects of DMOG in the endotoxemia model and suggesting DMOG may be utilising the same mechanism in the two models.

Discussion

There are overlaps in pathways active in hypoxia and inflammation (31). Previous studies have clearly shown that inhibition of hydroxylases by DMOG not only affects the HIF proteins but can also upregulate NF-κB, an observation confirmed in this report, thereby showing a distinct link between the pathways (13). In this study, we have further assessed the potential role for response evoked by hypoxia in the regulation of innate immune activation. We have shown that the hydroxylase inhibitor DMOG appears to tolerise cells to LPS activation, promote M2 polarization and subsequent upregulation of IL-10 by peritoneal B-1 cells, resulting in decreased susceptibility to endotoxemia.

Previous work has outlined the link between hypoxia and inflammatory conditions such as models of colitis, ischemia and certain cancers, with groups showing potential benefits using DMOG in the treatment of these conditions (5, 13, 32). A variety of mechanisms of action have been demonstrated for the action of DMOG, with groups showing regulation of cytokine production and adhesion molecules, apoptosis and NF-κB tolerance by DMOG (33, 34). Our data suggests two mechanisms through which DMOG is working in preventing endotoxemia: first, through tolerizing the peritoneal macrophages to NF-κB activation and promoting the generation of M2 MØ thereby attenuating the pro-inflammatory responses to LPS and, secondly, direct upregulation of IL-10 production, involving CREB activation as an example, specifically from peritoneal B-1 cells. We appreciate that CREB is just one possible mechanism linking hypoxia and IL-10, and to fully delineate the signalling underlying this response it would also be necessary to assess activation of other transcription factors such as AP-1 and Erk. The upregulation of NF-κB observed in response to DMOG treatment is likely to be direct activation of the p50 subunit. Pretreatment with DMOG has the effect of tolerising the mice to be refractory to subsequent challenge with LPS. In addition, recent work has shown that activation of the p50 NF-κB subunit actually inhibits M1 and drives M2 macrophage activation, a phenotype also associated with LPS tolerance (27). This has been demonstrated herein by the ability of DMOG to enhance M2 polarization by chitin, a known inducer of M2 activation (26).

Peritoneal B-1 cells are innate type cells, which are classically associated with production of IgM and IL-10 in response to infection or inflammatory stimuli. Recent work has demonstrated these cells are important in LPS-induced endotoxemia, with xid B-1 cell deficient mice showing higher mortality than WT mice (29). This suggests that the B-1 mediated IL-10 expression is important in protecting the mice against endotoxemia, which would support our data showing that the upregulation of IL-10 by DMOG plays a role in attenuating disease. These mechanisms support a protective immunoregulatory role for DMOG in a model of endotoxin shock resulting in decreased disease severity. Other studies have recently also linked these two observations demonstrating that B cells have the ability to drive macrophage polarization, specifically that IL-10 producing B-1 cells are able to induce M2 macrophage activation (35).

This project addresses the innate response to LPS induced inflammatory signaling, with DMOG modulating innate cell activation and downstream responses. As shown, DMOG upregulates expression of both NF-κB and HIF1α, it would therefore be important in the future to define the relative roles of NF-κB and HIF1α in LPS tolerance (6, 7). This would provide further mechanistic insights into the role of DMOG in innate activation. The experiments using polymicrobial sepsis however, demonstrate that while DMOG may attenuate LPS-induced systemic inflammation, it exacerbates the effects of systemic infection despite appearing to use the same mechanism. Polymicrobial sepsis, achieved by ligation and puncture of a section of the cecum, provides a more accurate model relevant to clinical sepsis. In this case sepsis is caused by gradual leakage of cecal contents into the

peritoneum, giving a model similar to sepsis caused by severe abdominal trauma (36). The cecal contents comprise a variety of bacterial flora resulting in activation of a variety of TLRs and other pattern recognition receptors (PRRs), therefore we hypothesise that while DMOG appears to be utilising the same mechanism in both models, due to the polymicrobial nature of the condition, this fails to protects against disease symptoms.

In summary, we have shown the hydroxylase inhibitor DMOG to be protective against acute systemic inflammation induced by the aseptic introduction of LPS leading to endotoxic shock. We also provide further insight as to the mechanisms utilized by DMOG and as such, show the mechanistic interplay between the pathways utilized by hypoxia and those utilized during innate activation. Studies have already demonstrated some benefit in using DMOG in more chronic inflammatory conditions, the interplay between cellular regulation in response to hypoxia or innate immunity presented herein, highlights this as an area for further research into the potential benefits of blocking prolyl-hydroxylases in more acute inflammatory conditions.

Supplementary Material

Refer to Web version on PubMed Central for supplementary material.

Acknowledgments

This work was supported by Science Foundation Ireland (07/IN1/B902) and Health Research Board.

References

1. Vincent JL, Sakr Y, Sprung CL, Ranieri VM, Reinhart K, Gerlach H, Moreno R, Carlet J, Le Gall JR, Payen D. Sepsis in European intensive care units: results of the SOAP study. Crit Care Med. 2006; 34:344–353. [PubMed: 16424713]
2. Danai PA, Sinha S, Moss M, Haber MJ, Martin GS. Seasonal variation in the epidemiology of sepsis. Crit Care Med. 2007; 35:410–415. [PubMed: 17167351]
3. Taylor CT. Interdependent roles for hypoxia inducible factor and nuclear factor-kappaB in hypoxic inflammation. J Physiol. 2008; 586:4055–4059. [PubMed: 18599532]
4. Kaelin WG Jr, Ratcliffe PJ. Oxygen sensing by metazoans: the central role of the HIF hydroxylase pathway. Mol Cell. 2008; 30:393–402. [PubMed: 18498744]
5. Cummins EP, Berra E, Comerford KM, Ginouves A, Fitzgerald KT, Seeballuck F, Godson C, Nielsen JE, Moynagh P, Pouyssegur J, Taylor CT. Prolyl hydroxylase-1 negatively regulates IkappaB kinase-beta, giving insight into hypoxia-induced NFkappaB activity. Proc Natl Acad Sci U S A. 2006; 103:18154–18159. [PubMed: 17114296]
6. Frede S, Stockmann C, Freitag P, Fandrey J. Bacterial lipopolysaccharide induces HIF-1 activation in human monocytes via p44/42 MAPK and NF-kappaB. Biochem J. 2006; 396:517–527. [PubMed: 16533170]
7. Rius J, Guma M, Schachtrup C, Akassoglou K, Zinkernagel AS, Nizet V, Johnson RS, Haddad GG, Karin M. NF-kappaB links innate immunity to the hypoxic response through transcriptional regulation of HIF-1alpha. Nature. 2008; 453:807–811. [PubMed: 18432192]
8. Walmsley SR, Print C, Farahi N, Peyssonnaux C, Johnson RS, Cramer T, Sobolewski A, Condliffe AM, Cowburn AS, Johnson N, Chilvers ER. Hypoxia-induced neutrophil survival is mediated by HIF-1alpha-dependent NF-kappaB activity. J Exp Med. 2005; 201:105–115. [PubMed: 15630139]
9. Peyssonnaux C, Cejudo-Martin P, Doedens A, Zinkernagel AS, Johnson RS, Nizet V. Cutting edge: Essential role of hypoxia inducible factor-1alpha in development of lipopolysaccharide-induced sepsis. J Immunol. 2007; 178:7516–7519. [PubMed: 17548584]
10. Thiel M, Caldwell CC, Kreth S, Kuboki S, Chen P, Smith P, Ohta A, Lentsch AB, Lukashev D, Sitkovsky MV. Targeted deletion of HIF-1alpha gene in T cells prevents their inhibition in

hypoxic inflamed tissues and improves septic mice survival. PLoS One. 2007; 2:e853. [PubMed: 17786224]

11. Hitchon CA, El-Gabalawy HS. Oxidation in rheumatoid arthritis. Arthritis Res Ther. 2006; 6:265–278. [PubMed: 15535839]
12. Rosenberger C, Solovan C, Rosenberger AD, Jinping L, Treudler R, Frei U, Eckardt KU, Brown LF. Upregulation of hypoxia-inducible factors in normal and psoriatic skin. J Invest Dermatol. 2007; 127:2445–2452. [PubMed: 17495954]
13. Cummins EP, Seeballuck F, Keely SJ, Mangan NE, Callanan JJ, Fallon PG, Taylor CT. The hydroxylase inhibitor dimethyloxalylglycine is protective in a murine model of colitis. Gastroenterology. 2008; 134:156–165. [PubMed: 18166353]
14. Hirota SA, Fines K, Ng J, Traboulsi D, Lee J, Ihara E, Li Y, Willmore WG, Chung D, Scully MM, Louie T, Medlicott S, Lejeune M, Chadee K, Armstrong G, Colgan SP, Muruve DA, MacDonald JA, Beck PL. Hypoxia-inducible factor signaling provides protection in Clostridium difficile-induced intestinal injury. Gastroenterology. 2011; 139:259–269. e253. [PubMed: 20347817]
15. Kamanaka M, Kim ST, Wan YY, Sutterwala FS, Lara-Tejero M, Galan JE, Harhaj E, Flavell RA. Expression of interleukin-10 in intestinal lymphocytes detected by an interleukin-10 reporter knockin tiger mouse. Immunity. 2006; 25:941–952. [PubMed: 17137799]
16. Magness ST, Jijon H, Van Houten Fisher N, Sharpless NE, Brenner DA, Jobin C. In vivo pattern of lipopolysaccharide and anti-CD3-induced NF-kappa B activation using a novel gene-targeted enhanced GFP reporter gene mouse. J Immunol. 2004; 173:1561–1570. [PubMed: 15265883]
17. Saunders SP, Barlow JL, Walsh CM, Bellsoi A, Smith P, McKenzie AN, Fallon PG. C-type lectin SIGN-R1 has a role in experimental colitis and responsiveness to lipopolysaccharide. J Immunol. 2010; 184:2627–2637. [PubMed: 20130211]
18. Mangan NE, Fallon RE, Smith P, van Rooijen N, McKenzie AN, Fallon PG. Helminth infection protects mice from anaphylaxis via IL-10-producing B cells. J Immunol. 2004; 173:6346–6356. [PubMed: 15528374]
19. Chan G, Bivins-Smith ER, Smith MS, Yurochko AD. NF-kappaB and phosphatidylinositol 3-kinase activity mediates the HCMV-induced atypical M1/M2 polarization of monocytes. Virus Res. 2009; 144:329–333. [PubMed: 19427341]
20. Xue J, Thippegowda PB, Hu G, Bachmaier K, Christman JW, Malik AB, Tiruppathi C. NF-kappaB regulates thrombin-induced ICAM-1 gene expression in cooperation with NFAT by binding to the intronic NF-kappaB site in the ICAM-1 gene. Physiol Genomics. 2009; 38:42–53. [PubMed: 19351910]
21. Takeda K, Ichiki T, Narabayashi E, Inanaga K, Miyazaki R, Hashimoto T, Matsuura H, Ikeda J, Miyata T, Sunagawa K. Inhibition of prolyl hydroxylase domain-containing protein suppressed lipopolysaccharide-induced TNF-alpha expression. Arterioscler Thromb Vasc Biol. 2009; 29:2132–2137. [PubMed: 19762779]
22. Biswas SK, Lopez-Collazo E. Endotoxin tolerance: new mechanisms, molecules and clinical significance. Trends Immunol. 2009; 30:475–487. [PubMed: 19781994]
23. Fitzpatrick SF, Tambuwala MM, Bruning U, Schaible B, Scholz CC, Byrne A, O'Connor A, Gallagher WM, Lenihan CR, Garvey JF, Howell K, Fallon PG, Cummins EP, Taylor CT. An intact canonical NF-kappaB pathway is required for inflammatory gene expression in response to hypoxia. J Immunol. 2011; 186:1091–1096. [PubMed: 21149600]
24. Gordon S, Taylor PR. Monocyte and macrophage heterogeneity. Nat Rev Immunol. 2005; 5:953–964. [PubMed: 16322748]
25. Mantovani A, Locati M. Orchestration of macrophage polarization. Blood. 2009; 114:3135–3136. [PubMed: 19815678]
26. Satoh T, Takeuchi O, Vandenbon A, Yasuda K, Tanaka Y, Kumagai Y, Miyake T, Matsushita K, Okazaki T, Saitoh T, Honma K, Matsuyama T, Yui K, Tsujimura T, Standley DM, Nakanishi K, Nakai K, Akira S. The Jmjd3-Irf4 axis regulates M2 macrophage polarization and host responses against helminth infection. Nat Immunol. 2011; 11:936–944. [PubMed: 20729857]
27. Nizet V, Johnson RS. Interdependence of hypoxic and innate immune responses. Nat Rev Immunol. 2009; 9:609–617. [PubMed: 19704417]

28. Siewe L, Bollati-Fogolin M, Wickenhauser C, Krieg T, Muller W, Roers A. Interleukin-10 derived from macrophages and/or neutrophils regulates the inflammatory response to LPS but not the response to CpG DNA. Eur J Immunol. 2006; 36:3248–3255. [PubMed: 17111348]

29. Barbeiro DF, Barbeiro HV, Faintuch J, Ariga SK, Mariano M, Popi AF, de Souza HP, Velasco IT, Soriano FG. B-1 cells temper endotoxemic inflammatory responses. Immunobiology. 2011

30. Sica A, Porta C, Riboldi E, Locati M. Convergent pathways of macrophage polarization: The role of B cells. Eur J Immunol. 2011; 40:2131–2133. [PubMed: 20623553]

31. Eltzschig HK, Carmeliet P. Hypoxia and inflammation. N Engl J Med. 2011; 364:656–665. [PubMed: 21323543]

32. Zhao HX, Wang XL, Wang YH, Wu Y, Li XY, Lv XP, Zhao ZQ, Zhao RR, Liu HR. Attenuation of myocardial injury by postconditioning: role of hypoxia inducible factor-1alpha. Basic Res Cardiol. 2011; 105:109–118. [PubMed: 19597757]

33. Frede S, Stockmann C, Winning S, Freitag P, Fandrey J. Hypoxia-inducible factor (HIF) 1alpha accumulation and HIF target gene expression are impaired after induction of endotoxin tolerance. J Immunol. 2009; 182:6470–6476. [PubMed: 19414801]

34. Hindryckx P, De Vos M, Jacques P, Ferdinande L, Peeters H, Olievier K, Bogaert S, Brinkman B, Vandenabeele P, Elewaut D, Laukens D. Hydroxylase Inhibition Abrogates TNF-{alpha}-Induced Intestinal Epithelial Damage by Hypoxia-Inducible Factor-1-Dependent Repression of FADD. J Immunol. 2011

35. Alexander C, Rietschel ET. Bacterial lipopolysaccharides and innate immunity. J Endotoxin Res. 2001; 7:167–202. [PubMed: 11581570]

36. Medina E. Murine model of polymicrobial septic peritonitis using cecal ligation and puncture (CLP). Methods Mol Biol. 2011; 602:411–415. [PubMed: 20012411]

Abbreviations used in this paper

MØ	macrophage
DMOG	dimethyloxallyl glycine

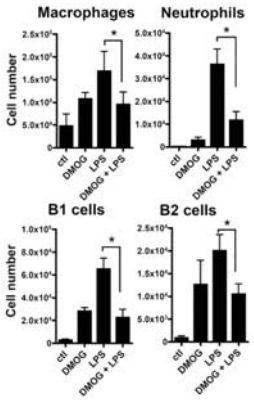

Figure 1. DMOG regulates LPS-induced NF-κB induction in peritoneal cells

NF-κB activation in peritoneal MØ (F4/80^{hi}CD11b^{hi}), neutrophils (L7-6G^{hi}CD11b^{hi}), B-1 cells (CD19^{+ve}CD5^{+ve}) and B-2 cells (CD19^{+ve}CD5^{-ve}), determined by NF-κB eGFP expression. Mice were treated with DMOG (8 mg/mouse), LPS (10 mg/kg) and DMOG (8 mg/mouse) 2 hours prior to LPS (10 mg/kg), peritoneal cells were collected 1 hour after LPS treatment. Data is representative of three separate experiments with 5 mice per group (mean +/- SEM, * P>0.05).

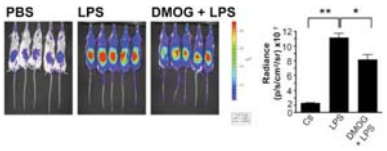

Figure 2. DMOG attenuates LPS-induced NF-κB activation *in vivo*

NF-κB activation visualized by luciferase activity, with the color indicative of the level of NF-κB activation, was assessed in whole adult mice in response to LPS stimulation with and without DMOG treatment with quantification of luciferase activity in response to i.p. injection of luciferin (150 mg/kg). Data is representative of three separate experiments with 5 mice per group (mean +/- SEM, * $P>0.05$, * $P<0.001$).

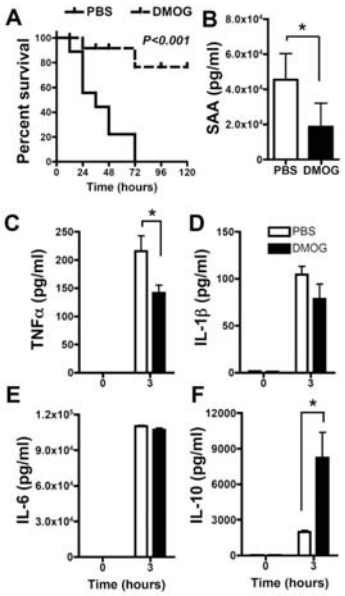

Figure 3. DMOG decreases mortality in LPS-induced endotoxin shock

(**A**) Survival of mice receiving LPS-induced shock with and without DMOG. Shock was induced in groups of male BALB/c mice by intra-peritoneal injection of 10 mg/kg LPS, groups received either LPS alone or 8 mg DMOG 2 hours prior to LPS. Mice were scored every 3 hours for 24 hours. (**B**) Levels of serum SAA were quantified by ELISA at 3 hours post LPS treatment. (**C**-**F**) Serum cytokines (TNFα (**C**), IL-1β (**D**), IL-6 (**E**) and IL-10 (**F**)) were quantified by MSD multiplex cytokine array 3 hours post LPS treatment. Data are representative of three separate experiments of 5 mice per group (mean +/- SEM, * *P*>0.05).

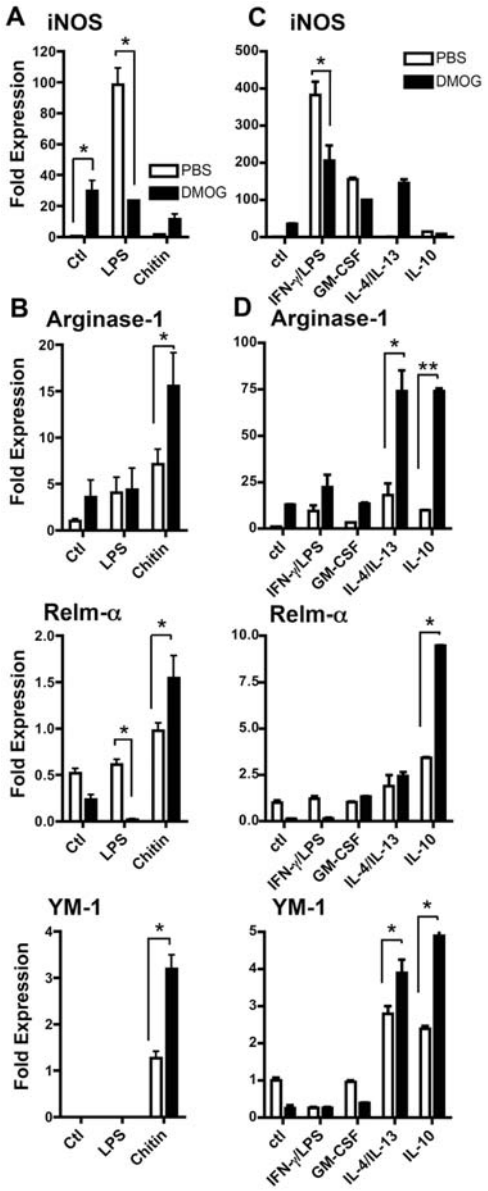

Figure 4. DMOG promotes M2 polarization in peritoneal macrophages

mRNA expression of M1 (**A**) and M2 (**B**) markers in peritoneal cells. Male BALB/c mice were given DMOG (8 mg/mouse) 2 hours prior to LPS (10 mg/kg) or chitin i.p. Peritoneal cells were collected by lavage 6 hours after LPS treatment and 48 hours after chitin treatment and cDNA prepared. mRNA expression of cultured peritoneal macrophages polarised to M1 by either GM-CSF (10 ng/ml) or a combination of LPS (10 μgml) and IFNγ (10 ng/ml) (**C**) and M2 by either IL-10 (10 ng/ml) or a combination of IL-4 (10 ng/ml) and IL-13 (10 ng/ml) (**D**). Cells were stimulated with DMOG for 2 hours prior to polarisation overnight, cDNA was prepared from the collected cells. RT-PCR was run using probes for Arg-1, Relm-α, YM1 and iNOS. Date expressed as fold expression was calculated comparing to GAPDH as a housekeeping gene. Data are representative of three independent experiments (mean +/- SEM, * $P<0.05$).

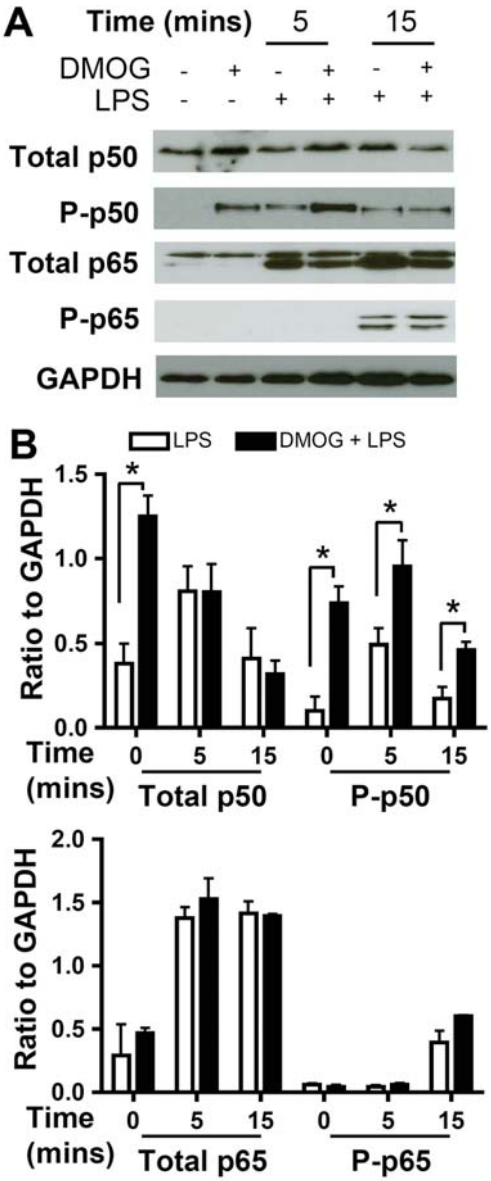

Figure 5. DMOG upregulates p50 in peritoneal MØ *in vitro*

(**A**) Whole cell extracts were prepared from peritoneal MØ cultured with DMOG (1 mM) for 2 hours prior to LPS (10 ng/ml) for 5, 15 and 30 minutes. Western blots were run with antibodies against total p50 and phosphorylated (P) p50, total p65 and phosphorylated (P) p65, GAPDH was used as a loading control. Densitometry was performed comparing each probe to the corresponding GAPDH band (**B**). Data are representative of 3-5 mice per group (mean +/- SEM, * $P>0.05$).

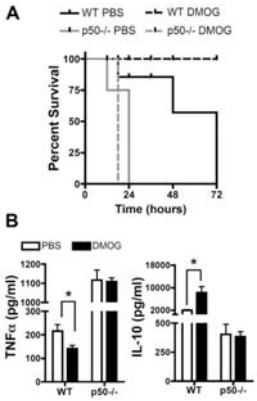

Figure 6. DMOG treatment does not protect p50$^{-/-}$ mice from LPS-induced endotoxemia

(**A**) Survival of p50$^{-/-}$ and WT mice receiving LPS-induced shock with and without DMOG. Shock was induced in groups of mice by intra-peritoneal injection of 10 mg/kg LPS, groups received either LPS alone or 8 mg DMOG 2 hours prior to LPS. Mice were scored every 3 hours for 96 hours. (**B**) Levels of serum TNFα and IL-10 were quantified by ELISA at 3 hours post LPS treatment. Data are representative of two separate experiments of 5 mice per group (mean +/- SEM, * $P<0.05$).

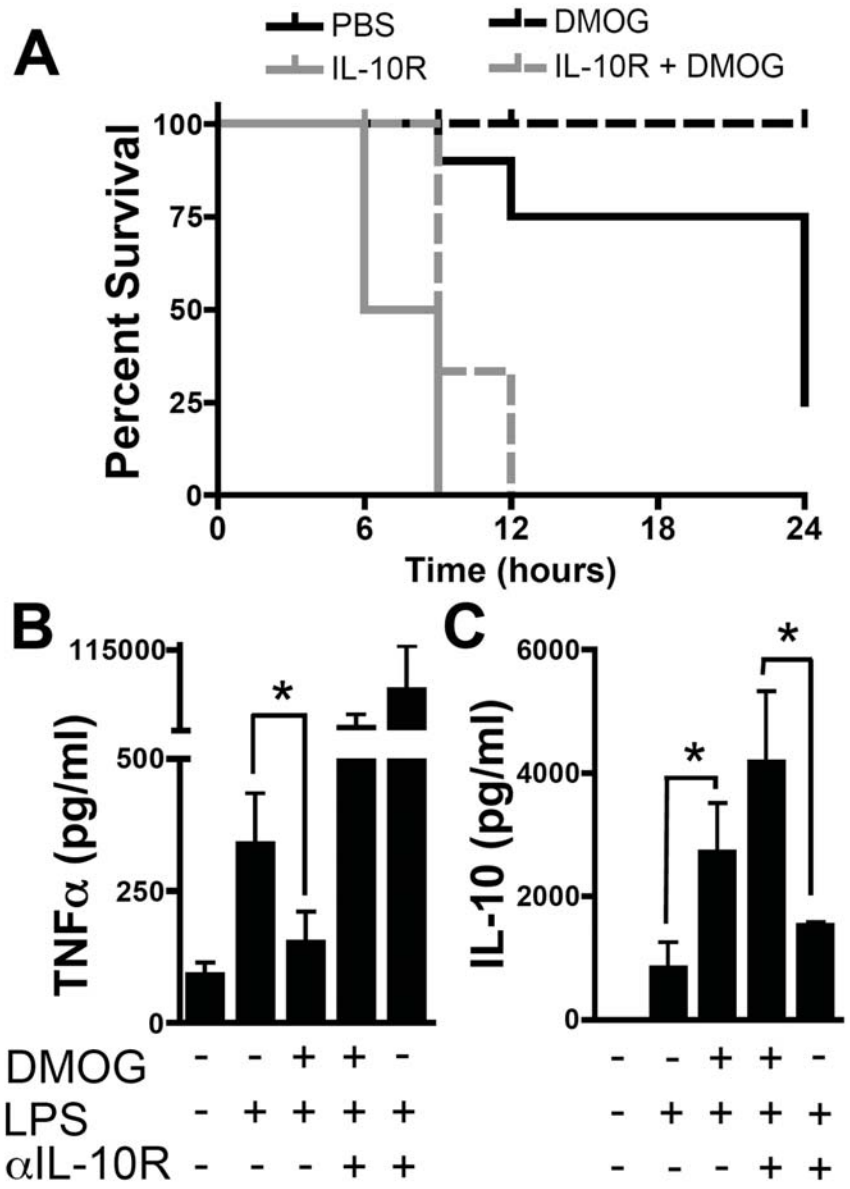

Figure 7. Protective effects of DMOG in LPS-induced endotoxin shock are blocked in mice treated with an IL-10R blocking antibody

(**A**) Survival of mice receiving an IL-10 receptor blocking antibody prior to LPS-induced shock with and without DMOG. Shock was induced in groups of male BALB/c mice by intra-peritoneal injection of 10 mg/kg LPS, groups received either anti-IL-10R alone, LPS alone, 8 mg DMOG 2 hours prior to LPS or anti-IL-10R 3 hours and DMOG 2 hours prior to LPS treatment. Mice were scored every 3 hours for 24 hours. (**B, C**) Serum cytokines (TNFα and IL-10) were quantified by MSD multiplex cytokine array 3 hours post treatment with LPS. Data are representative of 3-5 mice per group (mean +/- SEM, * P>0.05)

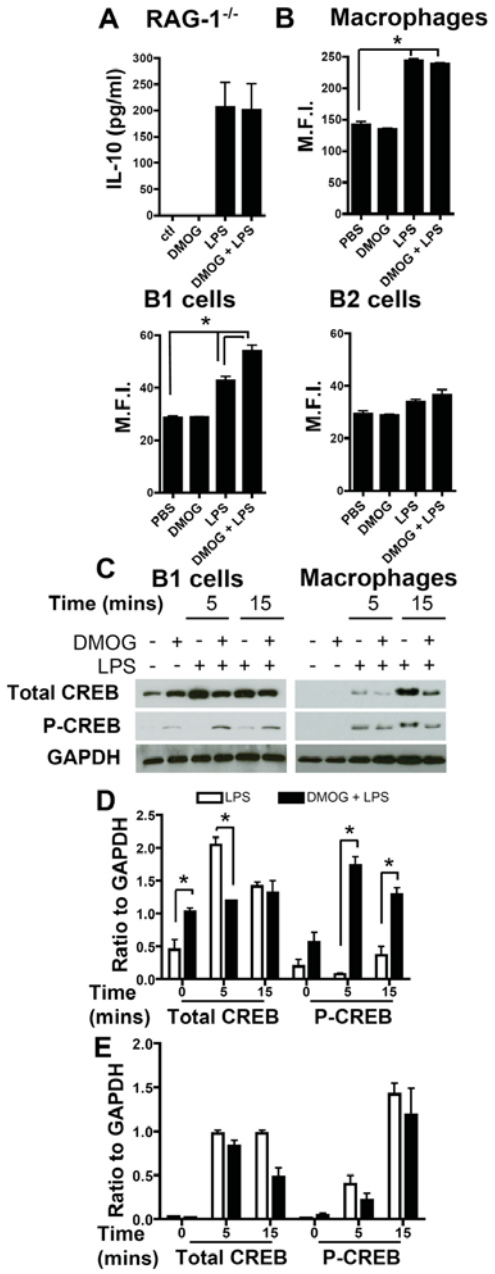

Figure 8. The cellular source of IL-10 in response to DMOG is peritoneal B-1 cells

(**A**) IL-10 levels in RAG mice after LPS-induced shock. Shock was induced in groups of male RAG mice by intra-peritoneal injection of 10 mg/kg LPS groups received either PBS or DMOG (8 mg/mouse) 2 hours prior to LPS treatment. Serum was collected 3 hours after LPS treatment and IL-10 levels were quantified by ELISA. (**B**) IL-10 expression in peritoneal MØ ($F4/80^{hi}CD11b^{hi}$), B-1 cells ($CD19^{+ve}CD5^{+ve}$) and B-2 cells ($CD19^{+ve}CD5^{-ve}$), determined by IL-10 eGFP expression and presented as MFI. Mice were treated with DMOG (8 mg/mouse), LPS (10 mg/kg) and DMOG (8 mg/mouse) 2 hours prior to LPS (10 mg/kg), peritoneal cells were collected 2 hours after LPS treatment. (**C**) Whole cell extracts were prepared from peritoneal MØ and isolated B1 cells cultured with DMOG

(1 mM) for 2 hours prior to LPS (10 ng/ml) for 5 and 15 minutes. Western blots were run with antibodies against total CREB and phosphorylated (P) CREB, GAPDH was used as a loading control. Densitometry was performed for B-1 cells (**D**) and macrophages (**E**), comparing each probe to the corresponding GAPDH band. Data are representative of 3-5 mice per group (mean +/- SEM, * $P>0.05$).

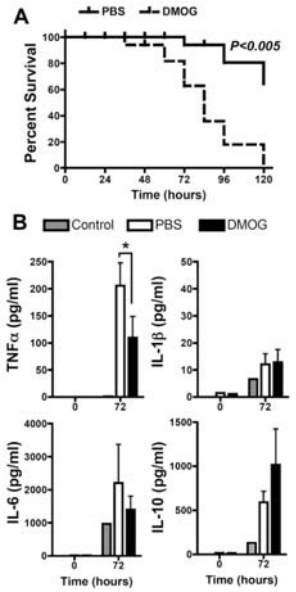

Figure 9. DMOG exaggerates disease and morbidity in CLP-induced sepsis

(**A**) Survival of mice receiving CLP-induced sepsis with and without DMOG. Sepsis was induced in groups of male BALB/c mice by ligation and puncture of a small section of the cecum, groups received either surgery alone or received 8 mg DMOG 2 hours prior to surgery. Mice were scored every 12 hours for 120 hours. (**B**) Serum cytokine levels in mice 72 hours after surgery. Data are representative of 19-21 mice per group (mean +/- SEM, * $P>0.05$).